PROCEEDINGS, Nineteenth Workshop on Geothermal Reservoir Engineering
Stanford University, Stanford, California, January 18-20, 1994
SGP-TR-147

NUMERICAL SIMULATION OF THE MORI GEOTHERMAL FIELD, JAPAN

Yukihiro Sakagawa[*1], Masahiro Takahashi[*1], Mineyuki Hanano[*1],
Tsuneo Ishido[*2] and Nobuhiro Demboya[*3]

[*1] Japan Metals and Chemicals Co., Ltd., Takizawa-mura, Iwate 020-01, Japan
[*2] Geological Survey of Japan, Tsukuba, Ibaraki 305, Japan
[*3] New Energy and Industrial Technology Development Organization, Toshima-ku, Tokyo 170, Japan
(now at Electric Power Development Co., Ltd., Chuo-ku, Tokyo 106, Japan)

ABSTRACT

A numerical study of the Mori geothermal field which consisted of a series of three-dimensional natural state modeling and history matching was carried out with porous models. Finally satisfactory fits both on temperature and pressure of the natural state and on pressure history caused by exploitation were obtained. The results indicate that the deep hot water ascends mainly through the fractures near the caldera wall and the fractures confined to some lithofaces, and some of the ascending hot water flows to the west from the caldera. A sketch of the geological structure, the way of making up the initial numerical model, the way of concluding free parameters, and results of calculations of natural state modeling and history matching for the best numerical model are presented.

INTRODUCTION

New Energy and Industrial Technology Development Organization (NEDO) started "the Development of Geothermal Reservoir Evaluation Technology Project" to develop the technology to analyze mass and heat transport in geothermal reservoirs, to predict the well production and to evaluate the optimum output power for the optimum geothermal development (e.g. Kitamura et al., 1988; Kawano et al., 1989).

As a part of the NEDO's project, this study was carried out to analyze the fluid flow and heat transport in the Mori geothermal field, Japan for the purposes of acquiring knowledge on structure of the geothermal system and of developing a reservoir model which reproduces the natural state and the reservoir behavior after the exploitation of the field to help the development of the field.

The Mori geothermal field is a liquid-dominated geothermal field located at the Nigorikawa Basin in the north Japan (Fig.1). In this field, the Mori geothermal power station (50 MWe) has been in operation since 1982 by Hokkaido Electric Power Inc. where Dohnan Geothermal Energy Co., Ltd., a subsidiary of Japan Metals and Chemicals Co., Ltd., is a steam supplier.

The geological structure of the field consists of the Pre-Tertiary Kamiiso Group, the Neogene Ebiyagawa Formation which unconformably overlies the Kamiiso Group and Quaternary caldera fill deposits composed of pyroclastics by caldera eruption, lake deposits, and andesite intrusions, as shown in Fig.2 (e.g., Sato, 1988; Ando et al., 1992; Kurozumi and Doi, 1993). The shape of the caldera has been confirmed by drilling and the three-dimensional gravity analysis (Kondo et al., 1993). The geothermal fluid is formed by simple mixing of heated meteoric water with deep hot water, with the latter having a large component of magmatic and/or altered sea water (e.g., Yoshida, 1991; Sato et al., 1992) . Fractures near the caldera wall and fractures confined to some lithofaces in the Ebiyagawa Formation and the Kamiiso Group are regarded as main conduits of hot up flow (Akazawa et al., 1993).

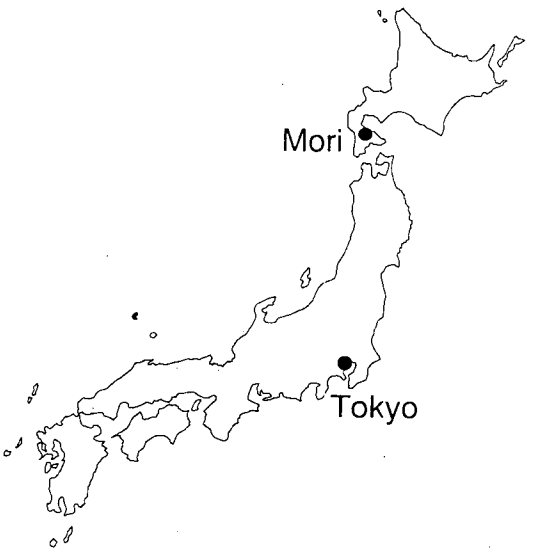

Fig.1 Location of the Mori geothermal field

In this study, three-dimensional natural state modeling, history matching, and prediction were carried out with porous models. The study proceeded on aiming at good matches both about temperature and pressure distribution of natural state and about reservoir pressure history measured in wells, with a single model. In this study we used SING-II, one of the NEDO's reservoir simulators, which is capable of analyzing three-dimensional transient mass and heat transport in porous or fractured media (e.g. Tsutsui et al., 1991).

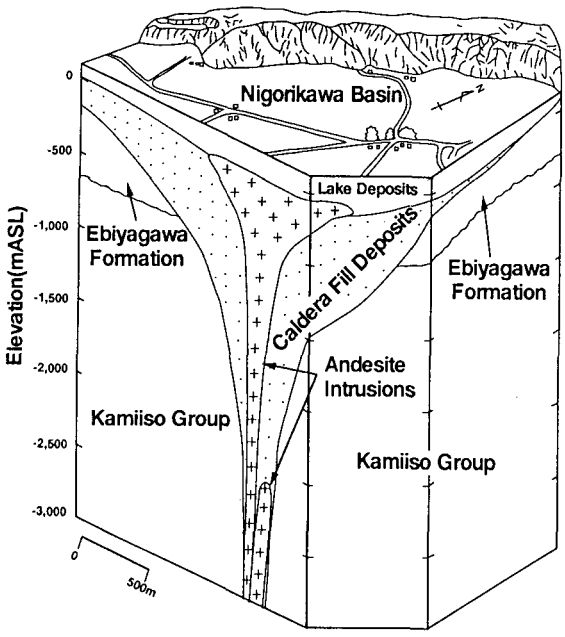

Fig.2 Schematic geological structure of the Mori field (modified from Kurozumi and Doi, 1993)

STUDY AREA AND GRID GEOMETRY

Since the horizontal shape of the caldera wall which makes the main conduit of fluid flow is rectangular in the depth, and the direction of its major axis is northeast–southwest, the grids were directed to northeast–southwest. The horizontal study area was 11.4km along northeast–southwest and 11.3km along northwest–southeast, and was divided into 14 x 14 grids (Fig.3). This area covers the Nigorikawa Basin and the mountainous area around the Nigorikawa Basin. It also includes wide area west of the Nigorikawa Basin, such as the Kaminoyu and Santai area, since the hydrothermal system of the Mori field was thought to extend mainly to the west (Kato and Takahashi, 1993). This extension of the hydrothermal system to the west was inferred from the facts that the hot area, centered on the caldera, extends to the west and that the reservoir pressure of the Kaminoyu and Santai area located in the west of the basin is essentially the same as that in the Mori field as shown in Fig.11.

The vertical study area was 3,900 m, from 100 mASL which is the approximate elevation of the ground surface of the Nigorikawa Basin to −3800 mASL. It was divided into 19 layers (Fig.4) to express the fractures confined to the upper part of limestone and chert in the Kamiiso Group, since a core fracture study shows that the deep fluid flows laterally in the fractures confined to the upper part of limestone and chert in the Kamiiso Group (Akazawa et al., 1993).

ROCK PROPERTIES

The values of porosity, rock density, thermal conductivity of rock, heat capacity of rock, and the values of permeability imposed to an initial model were given to each geological structure element or lithoface. The porosity was decided based on the analysis result of the electric log by the Archie's equation (Sunshine Project Promotion Headquarters, 1980). The rock density and thermal conductivity of rock were decided based on the core data; rock density ranges from about 2,300 to about 2,700 kg/m^3, and thermal conductivity about 1.4 to about 4.5 W/m·K. The heat capacity of rock was decided as 1,130 J/kg·K all over the area.

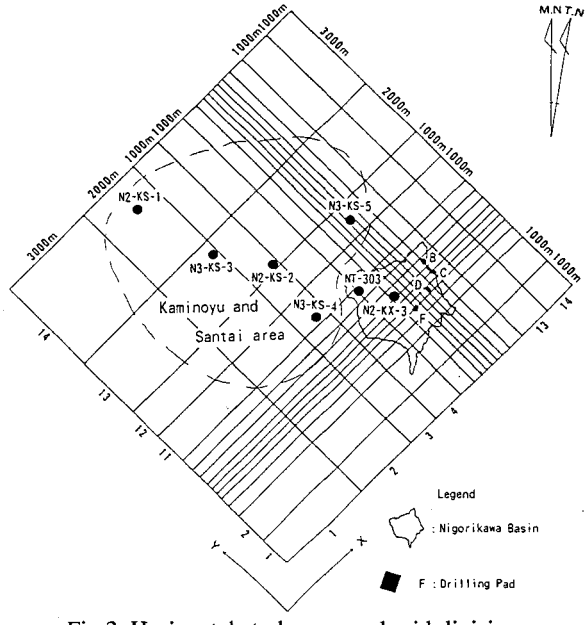

Fig.3 Horizontal study area and grid division

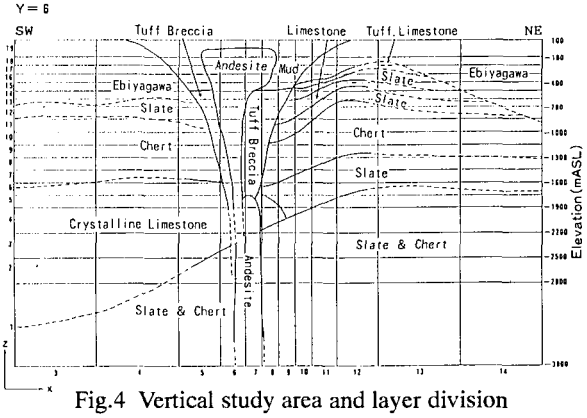

Fig.4 Vertical study area and layer division

With respect to the distribution of permeability given to the initial model, the geological structure was classified to some lithofaces, domains in which the fractures dominate, caldera wall and others, based on the results of such as chemical analysis of fluid, temperature profiles in wells and the results of core fracture study. The permeability of each grid was then decided by its class (e.g. horizontal permeability of the grids classified to Ebiyagawa Formation is 10^{-15}m^2 everywhere).

BOUNDARY AND INITIAL CONDITIONS

The top boundary was opened with respect to mass and heat flow. To permit the fluid flow we imposed a pressure distribution to the boundary surface. The pressure distribution was set heterogeneous; the boundary which has the higher elevation of the ground surface has the greater boundary pressure to account for the effect of the

mountainous area around the Nigorikawa Basin. With the homogeneous boundary pressure distribution, low temperature area in the shallow part of the southern basin was not reproduced. To permit conductive heat flow at the top boundary, we extracted heat from the each upper-most grid. The extracted heat was adjusted automatically all the time to maintain the initial temperature of the upper-most grids. The temperature of each upper-most grid was decided with reference to results of temperature logs in static wells and temperature distribution of the one meter depth which was reported by Urakami and Nishida (1977).

With respect to the bottom boundary, conductive heat flux was imposed on the bottom surface as heat supply but was closed to mass flow. However, constant rate mass input was imposed to some grids in the lower-most layer to represent up-flow of the deep hot recharge. Location and amount of the mass input are described later. The conductive heat flux at the bottom boundary was set to be 0.2 W/m^2 except up-flow zone of the deep recharge. This value is based on the initial temperature gradient of the model.

Side boundaries were closed to conductive heat flow and mass flow. Theoretically, there is no geothermal field with all of the side boundaries wholly closed, so that side boundaries are open though their boundary permeability is very small (e.g. order of 10^{-18} m^2). However, boundary conditions should not be sensitive to the result of simulation, if actual distributions of pressure or mass flux at the boundary can not be concluded. Therefore closed boundary conditions is thought to work well. This is the reason why we chose closed side boundary conditions.

The initial temperature distribution for the natural state modeling is linear for depth and laterally uniform; 20 °C at the top surface and 290 °C at the bottom surface. The bottom temperature is based on the hottest fluid temperature measured in one of the deepest production wells of the field. The initial pressure of each layer for the natural state modeling is hydrostatic with the uniform pressure distribution of 2.5 bars at the top surface (100 mASL).

RECHARGE GRIDS

At the first run of the natural state modeling, only one recharge grid was set in the lower-most layer just under the predominant producers since the feed points of them are located at almost the same point laterally. But with this recharge grid, the calculated hot area on each layer was laterally different from the measured one, so we shifted the recharge grid to cancel this gap. Moreover, only a small part of the depth of the system was warmed up with one recharge grid, so that an extreme amount of energy supply to the system was required to warm up the whole system. Thus, we made the recharge grids one of the free parameters, and we employed plural recharge grids laterally apart from its location of the initial model. Finally, the location of the recharge grids was concluded with X of 6 to 10, Y of 5 to 7 in the lower-most layer.

RECHARGE RATE

At the first run of the natural state modeling, the recharge rate of the deep hot water was set to be 13 kg/s which is equal to the total flow rate of hot springs through the ground surface of entire study area reported by Fukutomi et al. (1963). However, the result was not warm enough and temperature distribution of the natural state was not reproduced. Then we used 35 kg/s as the recharge rate based on the following analysis of the temperature profile of the well NT-303 located at the west of the Mori field (Fig.3).

The volume flux of steady state ascending flow in homogeneous half-infinite porous medium is obtained from the vertical temperature profile in the medium, when the hot water ascends homogeneously and one dimensionally from the infinite depth to the ground surface on which the temperature is kept constant. According to Turcotte and Schubert (1982, p.401), the temperature T (K) of the depth y (m) is

$$T=T_r-(T_r-T_o)\cdot\exp((\rho cv/\lambda)\cdot y) \qquad (1)$$

where T_r(K) is the temperature of the infinite depth, T_o(K) is the temperature at the ground surface, ρ(kg/m^3) is the density of fluid, c(J/kg·K) is the isobaric specific heat capacity of fluid, λ(W/m·K) is the thermal conductivity, and v(m^3/s·m^2) is the volume flux of the ascending flow.
Equation (1) can be reduced to

$$\log(T_r-T)=(\rho cv\cdot\log(e)/\lambda)\cdot y+\log(T_r-T_o) \qquad (2)$$

Thus, when the appropriate T_r is found, the relation of y and $\log(T_r-T)$ becomes linear, so that the volume flux of the ascending flow v can be calculated from the gradient of the graph.

All of the static temperature profiles of wells in the Mori field were investigated, and the profile of the well NT-303 was found to show the typical pattern of one dimensional ascending flow. Fig.5 shows the relation of the true vertical depth and $\log(T_r-T)$ for NT-303 with the tentative temperature of the infinite depth T_r of 230 °C (503 K). As the gradient of the linear part of the graph is -980 m/log-cycle, the volume flux of the ascending flow is 9.3 x 10^{-10} m^3/s·m^2, where ρ, c and λ are 919 kg/m^3, 4.18 x 10^3 J/kg·K, and 1.52 W/m·K, respectively.

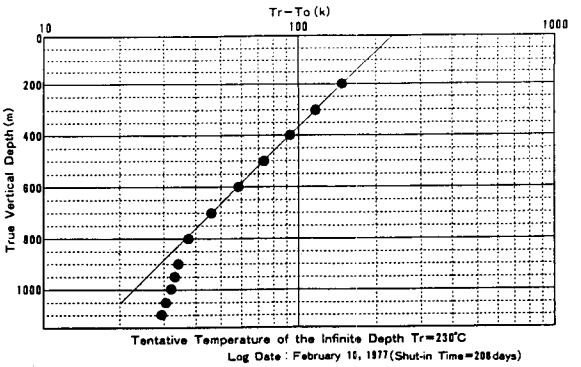

Fig.5 Analysis of the temperature profile of NT-303

Although this value was obtained by the analysis for the shallow part of NT-303, this value is regarded as the mean value of the whole study area because the well is located somewhat apart from the hottest part of the reservoir (Fig.9). The approximate flow rate of the hot water from the depth of the reservoir is obtained by multiplying this value by the area of the ascending flow. Since the domain of the ascending flow of the

hydrothermal convection in the Mori field is supposed to be about 6,300m x 6,400m (4.03×10^7 m^2 ; A), the mass rate of the ascending flow vρA is 34.5 kg/s. Therefore the recharge rate in the lower-most layer was finally decided as 35 kg/s. With respect to the temperature of the recharge, we employed 290 °C which is identical to the initial bottom-boundary temperature.

PERMEABILITY DISTRIBUTION

As described above, permeability distribution was firstly given in some classes based on the geological information. The permeability values were then adjusted to obtain a good fit basically as free parameters with the reference of the results of the natural state modeling and the history matching accounting for the results of pressure monitoring and pressure transient tests. The essential points to decide the permeability distribution are as follows.

(1) Permeability of the shallow grids in the mountainous region around the basin (grids which represent the Ebiyagawa Formation ; X=1 to 4, 13, 14, or Y=1, 2, 11 to 14) were reduced by one order of magnitude than their initial values. Since the pressure at the top boundary was specified taking into account the elevation of the ground surface, high pressure was given to the top boundary corresponding to the mountainous region as described above, so that the meteoric water is inclined to come down to the system. Therefore the permeability of the grids corresponding to the shallow part of the mountainous region around the basin had to be reduced to reduce the cold down flux and to warm up the entire system appropriately with a moderate heat input.

(2) Caldera fill deposits were divided into the shallow part with high permeability and the deep part with low permeability. Also, the concept of the shallow ground water aquifer was introduced. The cool part in the shallow portion of the southern basin was reproduced only with this shallow ground water aquifer. There exists small lateral gradient in the top boundary pressure given in the basin, since its pressure is high at the southern part and its pressure is low at the northern part due to the topographic gradient. Because of this lateral pressure gradient and high permeability of the aquifer, lateral cold water flow is induced and this makes the shallow part cool, while the low permeability below the aquifer guards all the other part against cooling by avoiding descent of the cold water to the deeper part of the system. This concept of the shallow ground water aquifer is supported by the fact that the cool part in the shallow portion of the southern basin was certified by wells mainly drilled in the F pad near the center of the basin as shown in the profile of measured temperatures of the well NF-2 in Fig.8. This concept is also supported by the fact that the temperature in the cool part proved by a well for water level monitoring in the southern basin and a test well in the southeastern basin is 10 to 12 °C which is lower by several tens degrees compared with temperature of the shallow ground water aquifer in other part of the basin (from the internal data of Dohnan Geothermal Energy Co., Ltd., 1992).

(3) The permeability values of caldera wall were adjusted according to the sizes of the relevant grids. If two grids of different size are considered for the caldera wall, and if they have the same permeability, the larger one has the higher transmissibility than the other in calculation. Thus, in deciding the permeability values of the grids which represent the caldera wall, we employed lower permeability for larger grids and higher permeability for smaller grids.

Fig.6 shows the final permeability distribution. Symbols in the figure denote the permeability class of each grid. For example, the deeper part of the caldera wall denoted by "W1" was given very large permeability of horizontally $1{,}000 \times 10^{-15}$ m^2 and vertically 100×10^{-15} m^2, while the Ebiyagawa Formation denoted by "Eb" was given relatively small permeability of horizontally 1×10^{-15} m^2 and vertically 0.1×10^{-15} m^2. Roughly speaking, the up flow zone of the deep recharge ("Up"; horizontally 10×10^{-15} m^2 and vertically 100×10^{-15} m^2), the deeper part of the caldera wall and the ground water aquifer ("Rs"; horizontally $4{,}000 \times 10^{-15}$ m^2 and vertically $4{,}000 \times 10^{-15}$ m^2) were given large permeability, and the deeper part of the caldera fill deposits ("Tf" and "An1"; horizontally 0.1×10^{-15} m^2 and vertically 0.01×10^{-15} m^2), the shallower part of the caldera wall ("W2"; horizontally 1×10^{-15} m^2 and vertically 0.1×10^{-15} m^2) and the Ebiyagawa Formation were given small permeability.

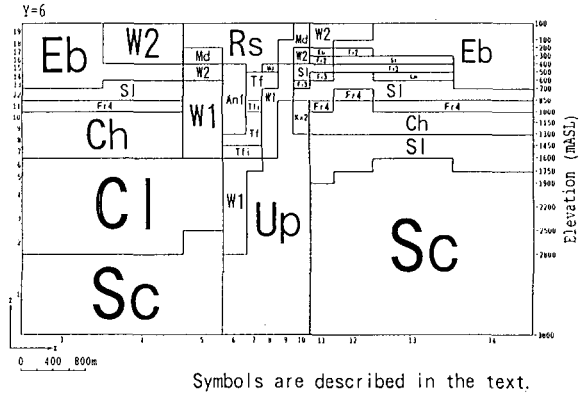

Symbols are described in the text.

Fig.6 Permeability distribution

RESULTS OF THE NATURAL STATE MODELING

The duration of the calculation was 20,000 years. This duration is regarded as reasonable since the volcanic activity which formed the caldera took place about 12,000 to 20,000 years ago, although the older volcanic activities also seems to have occurred (Sato, 1988). The flow of mass and heat approached steady state at the end of the run (Fig.7).

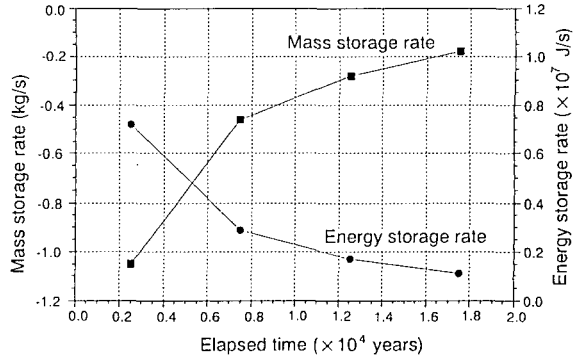

Fig.7 Change of mass and energy storage rate

The results of the natural state modeling were fitted to temperature profiles in wells and reservoir pressure measured before the exploitation in the Mori field. Fig.8 shows some of the temperature fits for the best model. Although the well N3-KS-4 was drilled after the start of exploitation, the well was thought to maintain its initial temperature because of distance from the Nigorikawa Basin. The calculated temperatures in Fig.8 are the temperatures of the grids in which the wells penetrate, and the minimum and maximum temperatures among the horizontally neighboring grids. The figure shows good fits in general. Especially the cool portion in the shallow southern part of the basin is clearly reproduced for the wells in the F pad. The temperature profiles of the wells NT-303 and N3-KS-4 which are drilled in the west part of the study area are also reproduced well. Thus, the lateral flow of the deep hot water to the west is well reproduced suggesting that the idea of the lateral flow towards west is feasible.

Fig.9 and Fig.10 show the calculated temperature distribution in plans and sections respectively. The figures show the extension of the hydrothermal system to the west. The cool part in the shallow portion of the southern basin is also shown in the figures.

Fig.11 shows the fit about the pressure distribution. The figure shows that the model well reproduced the pressure distribution of both the Mori field and the Kaminoyu and Santai area. This result also supports the idea of the lateral flow towards west. This result indicates that the average temperature of the whole study area is realistic enough. Therefore, the amount of the mass input and the conductive heat flux imposed to the deepest part of the study area are reasonable.

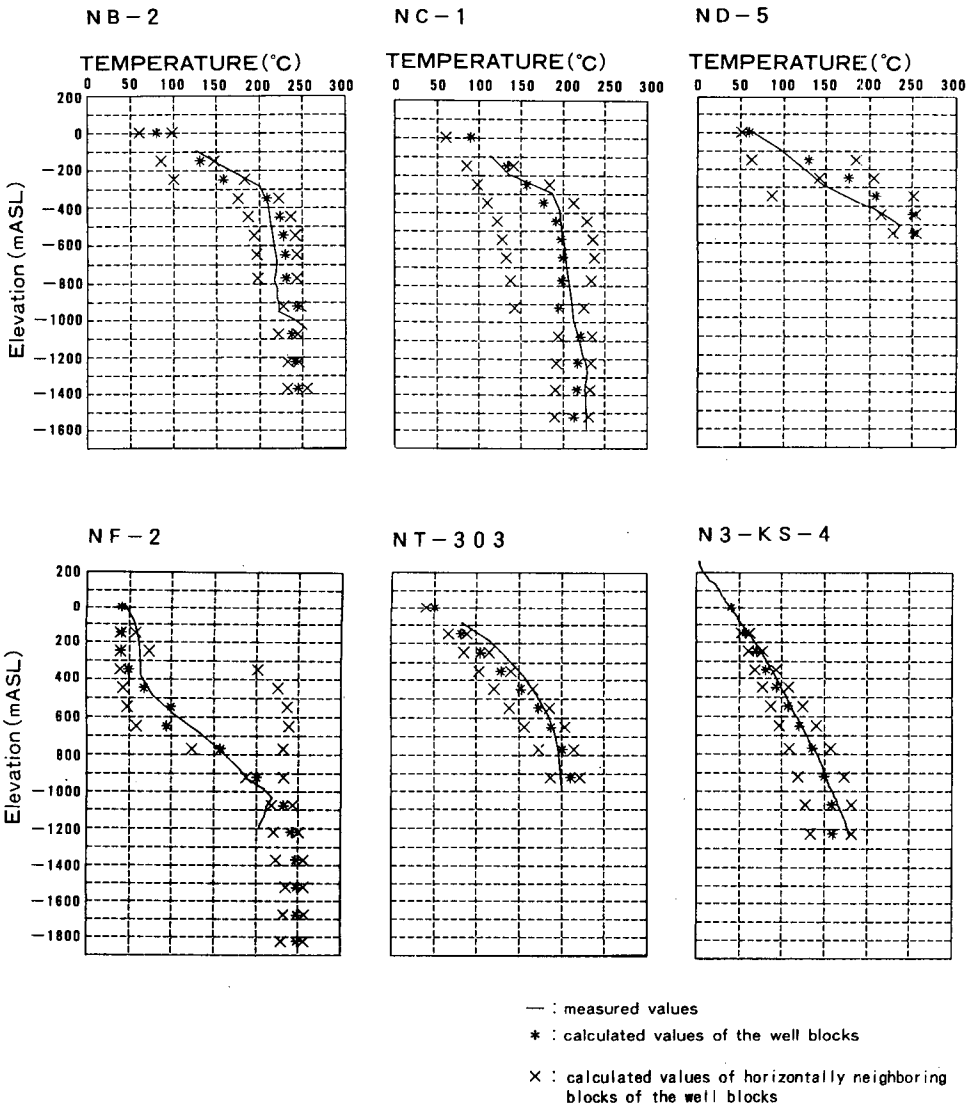

Fig.8 Some of the fits about the temperature profile of wells

RESULTS OF THE HISTORY MATCHING

Fig.12 shows some of the fits about pressure history. The calculated values in the figure were converted from the grid center depth to the depth of the feed point of the well using the temperature and the pressure of the grid. Two kinds of the measured values were used ; the results of the pressure logging in the static wells and the continuous observation of the pressure in the wells with the capillary tubes. The pressure values in the wells from the continuous observation with the capillary tubes were converted to the depth of the feed point using the temperatures and the pressures in the well. The figure shows that the fits of the pressure history are quite well.

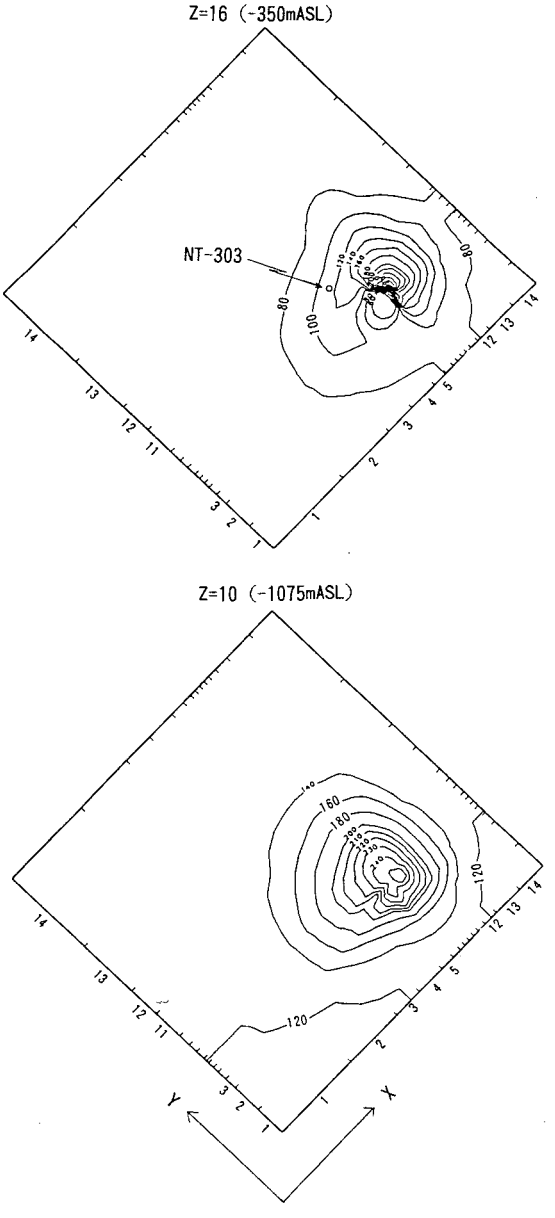

• Fig.9 Calculated temperature distribution (plan)

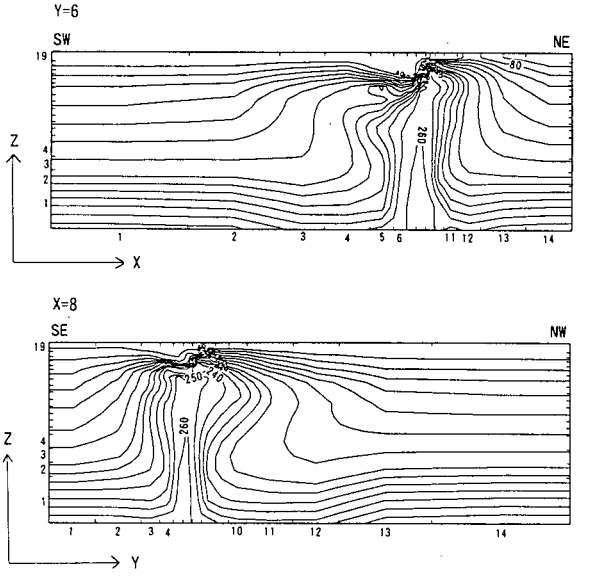

Fig.10 Calculated temperature distribution (vertical section)

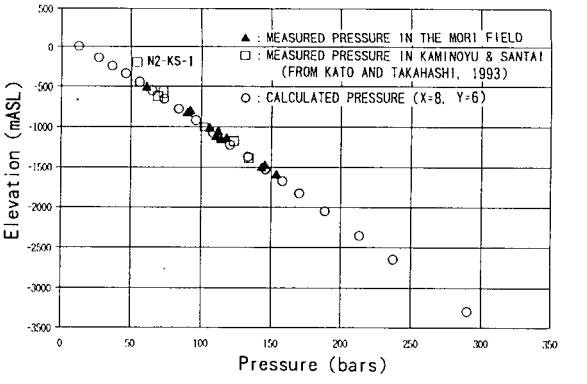

Fig.11 Fit about the pressure distribution

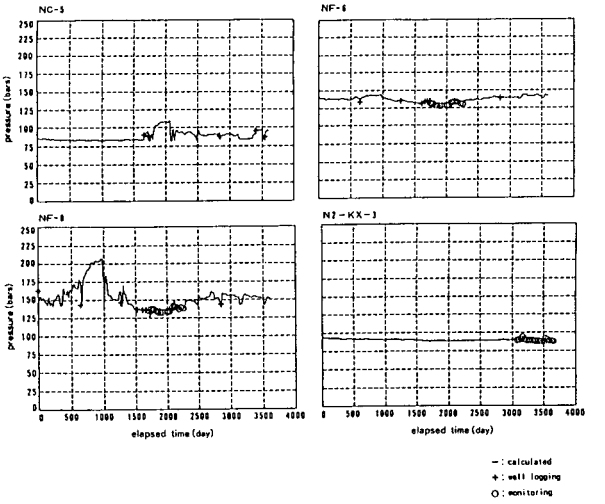

Fig.12 Some of the fits about the pressure history

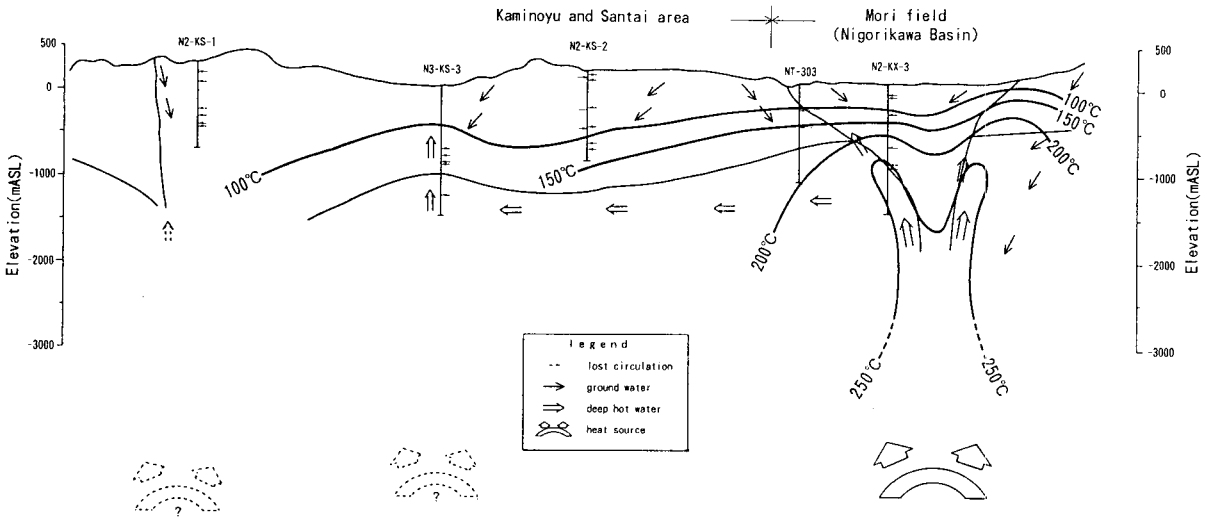

Fig.13 Conceptual model of schematic hydrothermal system of the Mori field and the Kaminoyu and Santai area (Kato and Takahashi, 1993; internal data of Dohnan Geothermal Energy Co., Ltd., 1992)

HYDROTHERMAL SYSTEM OF THE MORI FIELD

Based on the results of this study, we present a conceptual model of the hydrothermal system of the Mori geothermal field and the Kaminoyu and Santai area (Fig.13). The deep hot water of the Mori field consists of the meteoric water and the magmatic and/or altered sea water. It ascends from the depth of the Nigorikawa Basin and flows in the wide area including the Kaminoyu and Santai area. Some of the ascending fluid flows to the west in the Kamiiso Group because of the low permeability of the Ebiyagawa Formation overlying the Kamiiso Group (c.f. Fig.4). Also, because the permeability of the deeper part of the caldera fill deposits is low compared with that of the shallower part, the ground water does not descend so much and does not cool down the entire field. The up flow zone of the deep recharge had been thought to be rather small based on the distribution of the feed points of the predominant producers before this study, while now it has been found to be larger through this study. In this field, the reinjected water returned to the producers at the early periods of exploitation because of the short distances between producers and injectors. Thus, the distances have been enlarged to reduce the rate of return of reinjected water. Therefore, the possibility of the larger area of the up flow is an important implication to the future development of the Mori field.

CONCLUSIONS

The numerical model constructed in this study was proved to reproduce the temperature and pressure in the natural state and also the pressure change after the start of exploitation. Therefore the conceptual model that the deep hot water ascends mainly through the fractures near the caldera wall and the fractures confined to the upper part of limestone and chert in the Kamiiso Group, and some of the ascending hot water flows to the west from the caldera, was proved feasible. Also the concept of the shallow ground water aquifer was proved to well reproduce the cool part in the shallow portion of the southern basin.

ACKNOWLEDGEMENTS

This study was a part of the project "the Development of Geothermal Reservoir Evaluation Technology" assigned to Japan Metals and Chemicals Co., Ltd. (JMC) by New Energy and Industrial Technology Development Organization (NEDO). The authors sincerely thank NEDO and all members of the advisory committee for the project and for the sectional meeting about the Mori field for their support and suggestions. The authors thank NEDO for providing the data of the Kaminoyu and Santai area. The authors also thank NEDO, JMC and Dohnan Geothermal Energy Co., Ltd. for their permission to publish this paper.

REFERENCES

Akazawa, T., Kurozumi, H., Komatsu, R. and Demboya, N. (1993) Characteristics of Fractures in the Mori Geothermal Field. *Abstr. with Progr., Annual Meeting, Geothermal Research Society of Japan*, A7 (in Japanese).

Ando, S., Kurozumi, H., Komatsu, R. (1992) Structure and Caldera-fill Deposits of Nigorikawa Caldera. *Abstr., 29th International Geological Congress*, Vol.2, p.480.

Fukutomi, T., Fujiki, T., Sugawa, A., Ohtani, K., Wada, A. and Tokunaga, E. (1963) On the Hot Springs of Nigorikawa in Southern Hokkaido. *Geophys. Bull. Hokkaido University*, Vol.10, p.61-76 (in Japanese with English abstract).

Kato, H. and Takahashi, T. (1993) Hydrothermal System in the West of Nigorikawa Geothermal Field. *Abstr. with Progr., Annual Meeting, Geothermal Research Society of Japan*, A3 (in Japanese).

Kawano, Y., Maki, H., Ishido, T. and Kubota, Y. (1989) NEDO's Project on Geothermal Reservoir Engineering : A Reservoir Engineering Study of the Sumikawa Geothermal Field, Japan. *Proc., 14th Workshop on Geothermal Reservoir Engineering, Stanford University*, pp.55-59.

Kitamura, H., Ishido, T., Miyazaki, S., Abe, I. and Nobumoto, R. (1988) NEDO's Project on Geothermal Reservoir Engineering – A Reservoir Engineering Study of the Kirishima Field, Japan. *Proc., 13th Workshop on Geothermal Reservoir Engineering, Stanford University*, pp.47–51.

Kondo, T., Komatsu, R., Kurozumi, H. and Hanano, M. (1993) A Three–Dimensional Gravity Analysis at the Mori Geothermal Field, Hokkaido, Japan. *Proc., 88th Society of Exploration Geophysicists of Japan Conference*, p.490–495 (in Japanese).

Kurozumi, H. and Doi, N. (1993) Inner Structure of the Nigorikawa Caldera, *Progr. and Abstr., Volcanological Society of Japan*, No.2, p.14 (in Japanese).

Sato, K. (1988) Mori Geothermal Power Plant. *Geothermal Fields and Geothermal Power Plants in Japan, International Symposium on Geothermal Energy, Kumamoto and Beppu, Japan*, p.21–25.

Sato, K., Kasai, K. and Demboya, N. (1992) Isotopic Geochemistry in the Mori Geothermal Field. *Abstr. with Progr., Annual Meeting, Geothermal Research Society of Japan*, B7 (in Japanese).

Sunshine Project Promotion Headquarters (1980) Studies on Physicochemical Mechanism of Hot Water Injection. *Agency of Industrial Science and Technology, Ministry of International Trade and Industry*, pp.185 (in Japanese).

Tsutsui, M., Demboya, N., Nakai, Y., Oikawa, Y. and Ishido, T. (1991) Development of Three–Dimensional Unsteady Geothermal Reservoir Simulator, SING. *Abstr. with Progr., Annual Meeting, Geothermal Research Society of Japan*, P7 (in Japanese).

Turcotte, D.L. and Schubert, G. (1982) *Geodynamics*, Wiley, pp.450.

Urakami, K. and Nishida, Y. (1977) Heat Discharge Measurement and Geophysical Prospecting at Nigorikawa Basin, Northern Part of Komagatake. *Bull. Geol. Surv. Japan*, Vol.28, p.1–20 (in Japanese with English abstract).

Yoshida, Y. (1991) Geochemistry of the Nigorikawa Geothermal System, southeast Hokkaido, Japan. *Geochemical Journal*, Vol.25, p.203–222.